

WIND TUNNEL TESTS OF INNOVATIVE TAILPLANE CONFIGURATIONS

Fabrizio Nicolosi¹, Pierluigi Della Vecchia²

¹Full Professor, Dep. of Industrial Engineering, University of Naples "Federico II" ²Associate Professor, Dep. of Industrial Engineering, University of Naples "Federico II"

Abstract

The article deals with an experimental wind tunnel test campaign developed on a scaled model representative of a commercial jet tailplane. The main goal of aerodynamic tests is the test of an innovative tailplane geometry with forward sweep and with the application of a Leading Edge Extension (LEX) as stall control device. Tests have been performed on different geometries with positive and negative (forward) sweep angle. For the negative swept case several LEX with different shapes have been tested. Many visualization with tufts have been performed in order to highlight the tailplane stall path and the effect of LEX as stall control device. Several tests have been also performed with a boundary layer fence.

Keywords: innovative tailplane aerodynamics, wind tunnel tests, aircraft tailplane design, stall control

1. Introduction

In the next decades the air traffic will growth and the need of emission's reduction will be more and more demanding. This trend is represented by approximately 39,500 aircraft deliveries expected (passenger aircraft above 100 seats and freighters with a payload above 10t) between 2022 and 2041, being ~31,600 (80%) of narrow-body and ~7,900 (20%) of wide-body. Approximately 15,000 $(\sim 40\%)$ of those new deliveries will be to replace the current fleet, while the rest would be for growth. Conventional designs and solutions in aviation industry have already been widely investigated and optimized, hence it is time to study unconventional shapes and sizes, in order to improve the safety and environmental performances, be it reducing the weight and thus the fuel consumption. Nevertheless, these new shapes have never been investigated, therefore the studies start from scratch. These numbers point to a considerable growth of the aerospace industry, however, this expansion makes us wonder if environment preservation, reduction of emissions and sustainability is achievable for the aeronautic sector. Aviation contributes between 2% and 3% of world CO2 emissions. Moreover, environmental challenge go hand in hand with an economic point: the reduction of fuel consumption and operational costs. To this aim, airlines require the latest, most efficient and lowest-emission aircraft. In 2021, new generation aircraft represent just 20% of the fleet. By 2041, it is expected that this percentage grow up to 95%. Thus, it is crucial to investigate different technologies to produce a new aircraft that meets ACARE [1] requirements and improves profitability by reducing Direct Operating Costs (DOC), such as through the use of new material technologies [2]- [3].

Traditionally, horizontal tailplanes are designed with rearward sweep, reflecting the common configuration seen in conventional aircraft. However, researchers have begun to recognize the potential benefits of incorporating forward sweep in both wing and horizontal tailplane designs. This interest has grown in recent years as the aerodynamic and aeroelastic behavior of non-conventional aircraft configurations has become a focal point for developing new aeroelastic technologies.

Forward-Swept Horizontal Tail Planes (FSHTP) and Forward-Swept Wings (FSW) have shown

promise in enhancing aircraft performance, stability, control, and maneuverability. The surge in research in this area has been driven by advancements in computational techniques and materials science. Aerodynamic benefits of forward sweep, such as reduced drag divergence, improved stall characteristics, and better lift-to-drag ratios, have led to their adoption in various aircraft designs.

Krone [4] provides a historical overview of forward sweep, dating back to the early 1940s, and discusses both the advantages and challenges associated with this design. The importance of flight demonstrators in fully exploring the benefits of forward sweep is emphasized. Numerous studies have examined the divergence behavior of high-aspect-ratio, laminated composite forward-swept wings [5]-[9]. These studies highlight that aeroelastic tailoring is crucial for maximizing the benefits of positively swept wings.

Consequently, research efforts, such as those presented in [10] and [11], have introduced aeroelastic tailoring as a design process. These works utilize a process chain for aerostructural wing optimization to enhance aerodynamic, structural, and fuel efficiency while effectively controlling aeroelastic deformation in forward-swept wings.

The European Union has funded many projects to study these new designs, including the IMPACT project [12]. The cornerstone of this project is the improvement of the efficiency and effectiveness of LPA's "rear end" (tail planes and fuselage tail cone). IMPACT tackles all the challenges of the call JTI-CS2-2019-CfP10-LPA-01-80, "Rear fuselage and empennage shape optimization including anticing technologies".

To realize its ambition, IMPACT relies on a vast portfolio of competences from a consortium of 10 partners (from Austria, Italy, the UK and Canada), led and coordinated by the Austrian Institute of Technology (AIT). Among the goals of the project, one of the most important has been the aerodynamic and aerostructural optimization of the rear end (tailplanes). The work has been carried out through the development and application of innovative aerostructural optimisation methods for advanced rear ends (ARE), including the effects of the passive anti-ice coatings and devices, to minimize drag and include structural and aeroelastic constraints.

The aerodynamic performance of an horizontal tailplanes can be summarized with mainly two fundamental goals. The first one is the increase of the lift curve slope, which together with the HT longitudinal position will define the arm and the very important stabilizing contribution of the tailplane. The second aerodynamic goal is the maximum lift coefficient (negative, downward direction) which is very important in defining the low speed equilibrium of the aircraft (stall speed for the whole A/C) and the maneuver capabilities of the aircraft. Of course the previous aerodynamic characteristics should be accompanied by lowest drag and low compressibility effects in cruise at high Mach numbers.

The project will develop a tailplane that reaches higher angles of stall, introducing a forward sweep horizontal tailplane (FSHTP) [14]. This concept became a patent US 8,360,359 B2 in 2013 by Airbus [14], the team leader of IMPACT project. Having a larger stall angle allows to increase the maximum aerodynamic force for a given surface, or for the same maximum aerodynamic force, it reduces the tail surface, and therefore, drag and weight. Despite this drawback, some studies have investigated the possibility of exploiting the aerodynamic benefits of a forward-swept wing [15]-[16] proposing a solution to mitigate the coupling between flexional and torsional deformation by using aeroelastic tailoring techniques. In terms of structural sizing, aeroelasticity is less demanding for wings with a relatively low aspect ratio. Thus, in the case of horizontal tails, introducing negative sweep angles could be a viable solution to improve the performance of the rear end and empennage.

The aerodynamic advantages associated with an airfoil configuration with negative sweepback are well known, and can be summarized as follows:

a) Negative sweep angle results in less of a tendency for the flow to move along the direction of the wingspan, which leads to a reduction of the boundary layer global skin friction coefficient and, therefore, reducing the drag. In addition to this, a forward sweep wing allows to delay the stall. For positive sweep angle, the flow is from root to tip, decreasing the energy of the boundary layer in that zone which, as it has a higher local lift coefficient than the root zone, causes separation of the boundary layer with the resulting lift stalling at a smaller angle of attack than in the case of the negative sweepback wing. For negative sweep angle, the flow is from tip to root, therefore

the boundary layer is accumulated on the root which has a greater local surface, hence preventing the stall, allowing to reach higher angles of attack.

b) A swept wing is required to delay the compressibility effects when flying on the transonic regime [14]. Conventional assemblies show a positive sweepback due to structural reasons. The elastic deformation tends to decrease the local angle of attack for positive sweepback, naturally relieving the loads. For negative sweepback, the aeroelastic deformation tends to increase the local angle of attack, with the resulting increase in the aerodynamic lift gradient with the angle of attack. This increase of the lift gradient enhances the maneuverability and is desirable for a stabilizer surface, since it results in a greater dynamic response to turbulence and to vertical gusts making the stabilizer more efficient.

In spite of these aerodynamic advantages, negative sweep wings have some structural limitations that have limited their use and can be summarized as follows:

- c) The elastic deformation for sweepback wings tends to increase the local angle of attack, increasing the loads, which could lead to a possible divergence and structural failure. To avoid this, a reinforcement of the structure would be needed, which inevitably increases the weight. Furthermore, the increase of the lift gradient is usually considered as a drawback for commercial airplanes because it results in a greater dynamic response of the airplane to turbulence and to vertical gusts and, therefore, less comfort for passengers.
- d) The geometry of the negative sweepback wing complicates the integration of the landing gear into a low wing commercial airplane because the rear spar forms an angle of more than 90 degrees with the rear of the fuselage
- e) The flap type high lift systems lose aerodynamic efficiency due to the larger sweep angle of the trailing edge.
- f) Increasing the sweep angle has a similar effect as increasing the relative thickness of an airfoil, which deteriorates aircraft cruise performances in transonic region. Sweptback wings suffer less compressibility effects at high speed than forward sweep wings (wave drag)

However, the above-mentioned drawbacks apply mainly on the wings but not on stabilizer surfaces, which is the focus of this study. Therefore, a stabilizer surface with negative sweep angle would be more efficient (in regard to size, weight and drag) than an empennage with positive sweepback, having both their aerodynamic center at the same distance from the aerodynamic centre of the wing. The main advantage of a stabilizer surface with a negative sweep angle is that, having the aerodynamic centre at the same distance from the aerodynamic centre of the wing, it enables a structural configuration where the horizontal stabilizer is connected to the rear end of the fuselage without requiring a structural opening on the fuselage. The structural connection of the horizontal stabilizer to the aircraft fuselage is made between points of the front spar of the horizontal stabilizer and a fuselage frame, removing the requirement of a structural opening in a zone very affected by the loads of vertical and horizontal stabilizers. Thanks to this, the reinforcements required by the opening are no longer needed and can be suppressed, diminishing the structural weight.

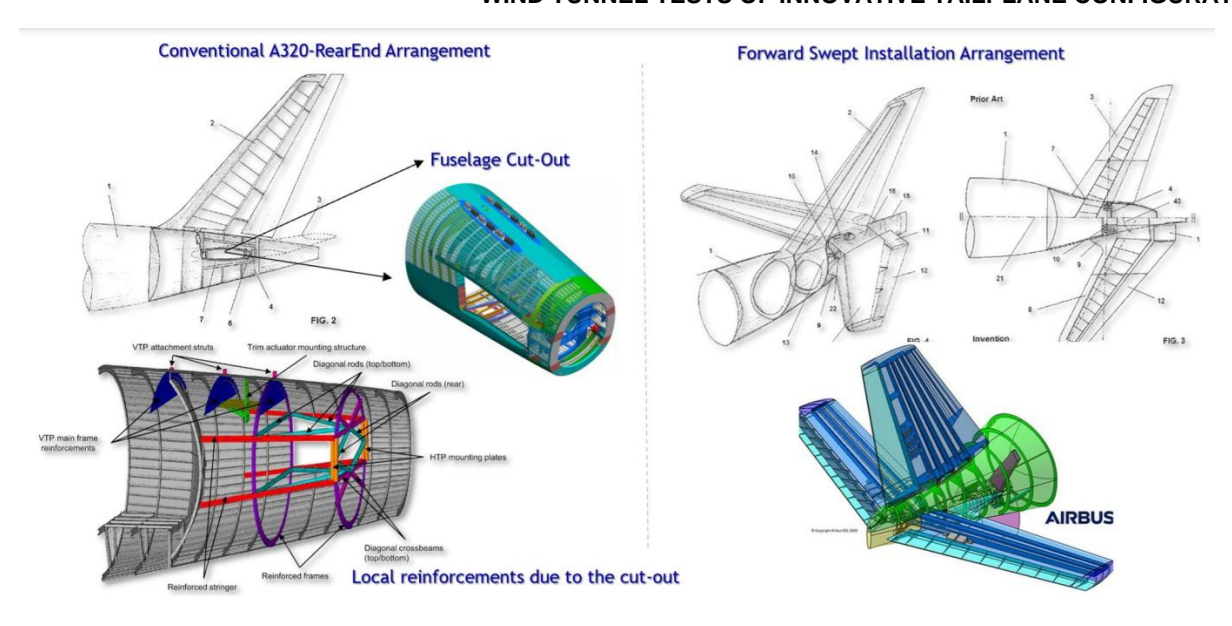


Figure 1: Conventional configuration (left) vs Non conventional configuration (right)

However, the aerodynamic performance of the isolated forward swept wing worsen when it is joined to the fuselage. The angle between the leading edge of the HTP and the fuselage triggers a flow separation that is larger than for the sweepback tail plane. In Figure 2 the CFD results concerning a conventional sweptback tailplane and an innovative forward swept tailplane analyzed both at an angle of attack of -8 deg. are shown. The forward swept tailplane at this angle of attack leads to a premature flow separation at tailplane-fuselage junction. This leads to the need of a passive stall control device.

For this reason, the leading edge of the horizontal stabilizer comprises a local extension in the flight direction of the aircraft, in the zone adjacent to the fuselage (see figure 3). The local extension preferably has an essentially triangular shape and is designed to offset the loss of airflow speed in the boundary layer of the fuselage, such that it prevents the formation of horseshoe vortexes around the root of this stabilizer surface at small angles of attack. The extension of the leading edge of the horizontal stabilizer surface in the zone adjacent to the aircraft fuselage is designed so that the radius of curvature of the leading edge of this extension is less than on the rest of the leading edge of the horizontal stabilizer, in order to provoke a controlled separation of the aerodynamic flow at high angles of attack of this surface in the form of a vortex that delays the generalized separation of the aerodynamic flow over this stabilizer surface, and therefore, increases the maximum angle of attack in which this stabilizer surface is effective.

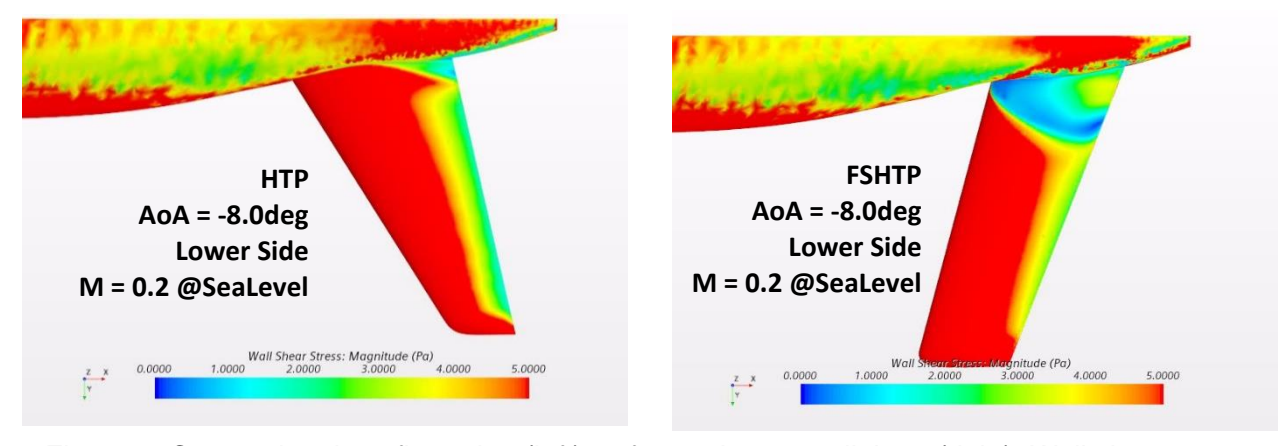
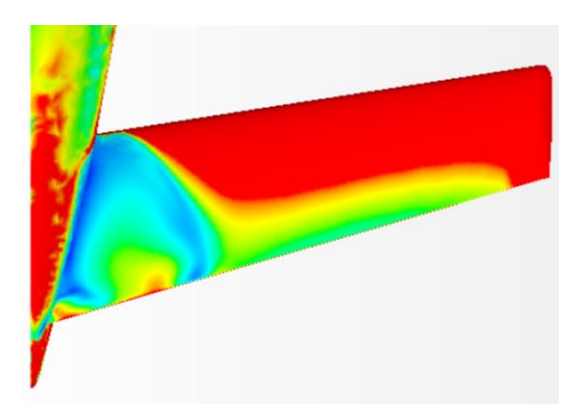


Figure 2: Conventional configuration (left) vs forward swept tailplane (right). Wall shear stress (indicates flow separation) at angle of attack of -8°.



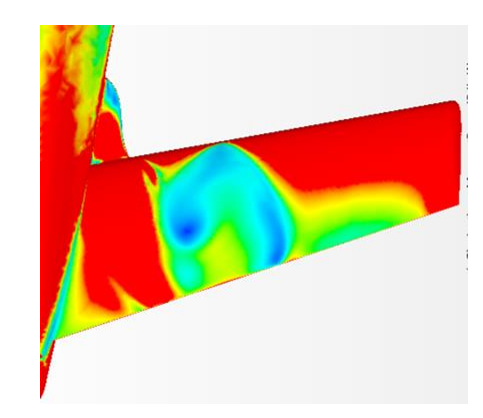


Figure 3: Forward swept tailplane aerodynamic behavior without LEX and with the application of a LEX (Leading Edge Extension device at an angle of attack of -10 deg.

2. Wind Tunnel Tests setup

2.1 Low-speed wind tunnel

The tests have been carried out in the main Low-speed wind tunnel of the Department of Industrial Engineering (DII) of University of Naples Federico II. This is a subsonic, closed circuit and test section tunnel. Figures 4.1a and 4.1b show a front and rear view of the facility where wind tunnel is operated.

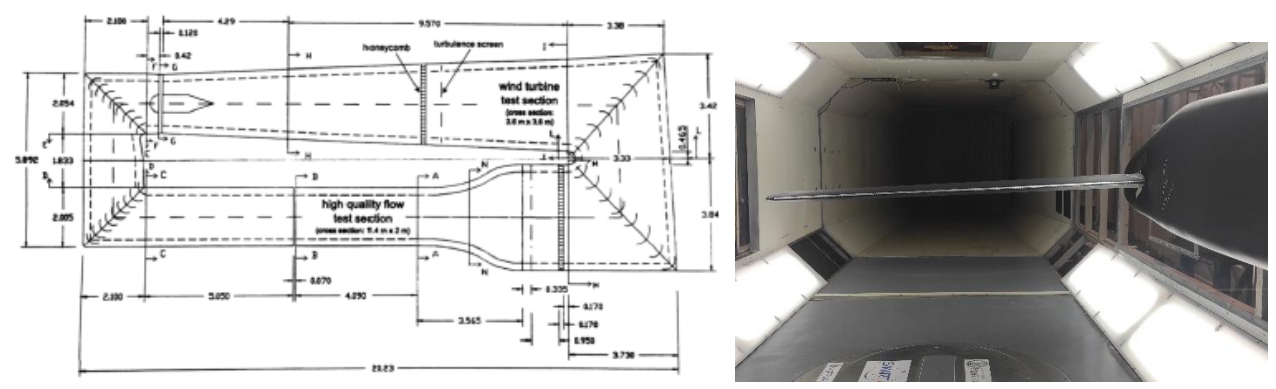


Figure 4: Low-speed wind tunnel of University of Naples "Federico II"

This subsonic tunnel has a maximum power o 150 kW, a turbulence level of 0.10% and a maximum wind speed of 50 m/s. The tests section dimensions are 2.0 m width for 1.4 m height, with smoothed corners, as also shown in Fig. 4. The test typology was the semi-model tests (as shown in Fig. 4), with a semi-model mounted on a side-wall and an external balance measuring aerodynamic forces. Tests have been performed at a wind-speed of about 35 m/s in order to contain forces (especially bending moment on the external balance).

2.2 Horizontal tailplane scaled model

The test model is composed by a fuselage (fixed on the wind tunnel wall) and the tailplane attached to the external balance. So the aerodynamic forces are measured only on the tailplane. The fuselage is manufactured in two parts using Smart Board GB-80 resin. The smaller part is positioned in the section in which the wing connects to the external balance in order to facilitate the assembly of both configurations (FSHTP and HTP), and slips in the bigger one through 2 slots, one in each face.

For the tested model (the tailplane) a scaled factor of 4.415 has been applied, leading to model dimensions shown in Figure 5. The tailplane semi-span is close to 1.5 m (1.52 m), while the "dummy" fuselage is a geometry which represents the real fuselage geometry only in the region close to the tailplane to lead to the same real scale interference on the tailplane. The fuselage has been shaped with a flat geometry ahead of the tailplane in order to guarantee more regular flow conditions in the tailplane junction area. Clearly, due to the scale chosen (in order to increase the Reynolds number) the fuselage could not be represented with the real geometry which would have been leading to much longer fuselage model going upstream of the test section inside the convergent. The tailplane model

has been conceived in three parts (see A, B and C in Figure 5 and Figure 6) to be assembled in order to be able to test a classical tailplane geometry with positive sweep (+30 deg) and a forward swept tailplane with a sweep angle of -10 deg. The tailplane area of the two tailplane is almost the same and the attachment to the balance is made in such a way to have almost the same pitching moment on the external balance (in one case negative pitching moment and in the other case negative pitching moment). As it is evident from the picture in figure 5, the geometry tested in the tunnel is mounted upside-down, so positive angle of attack will correspond to negative angle. In this way the weight of the model will balance the aerodynamic lift load which is directed upward.

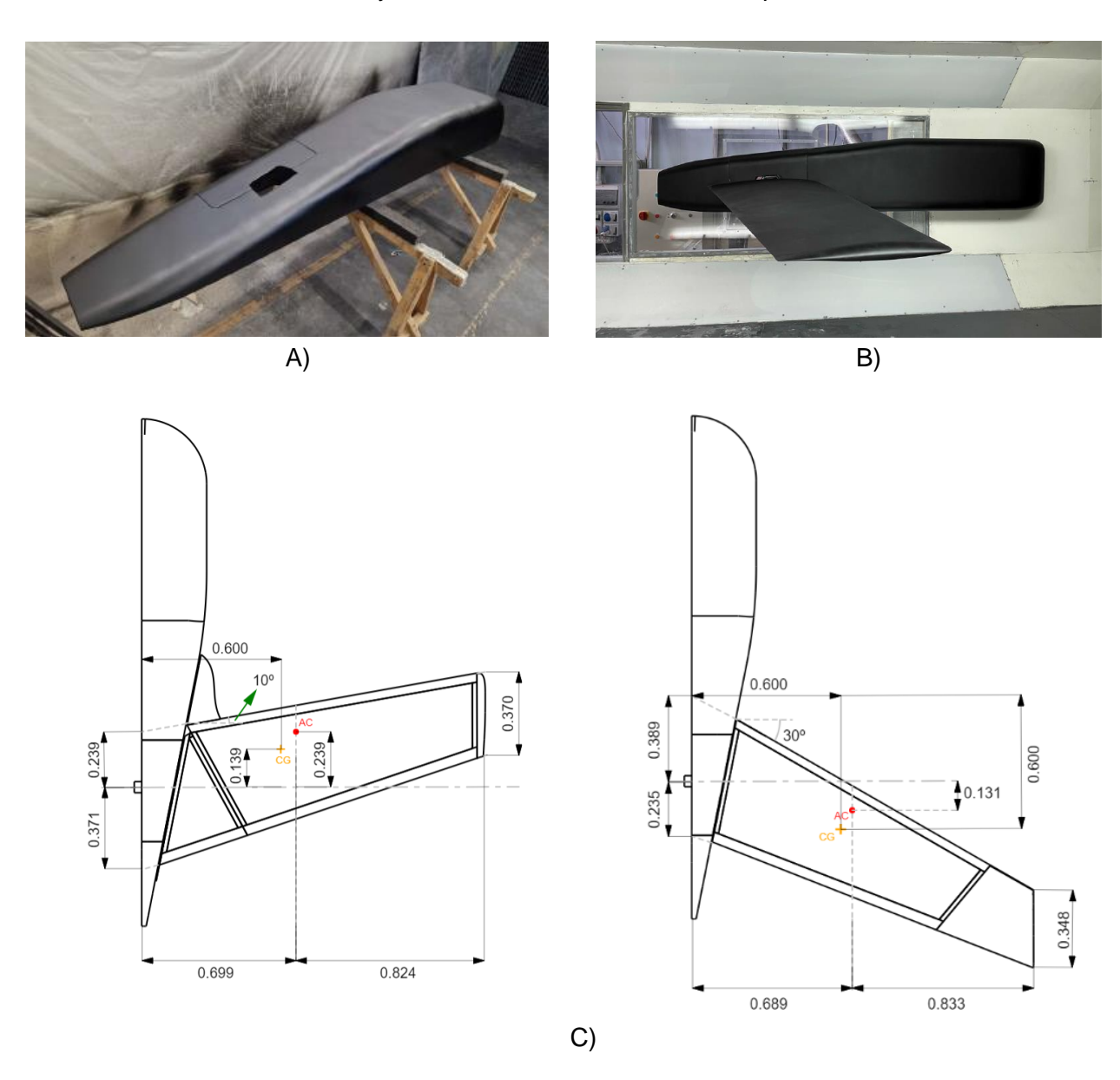


Figure 5: Tested tailplane models plus dummy fuselage model.

The tailplane main structure is made of 6082 series aluminum, with hardened steel pins DIN 6325 8x35 H6. The skin is manufactured using RenShape BM 5060 resin.

The model, for the configuration with forward sweep angle (left in Figure 5) is also equipped with a removable series of Leading Edge stall control device (LEX) that are attached through several aluminum pins to the tailplane model (part B). Together with the forward sweep tailplane without any device, 5 different LEX shapes have been tested to see the effect of different LEX geometries on the stall of the tailplane. The LEX different shape are shown in Figure 7.

HTP	FSHTP
1.522	1.523
0.624	0.610
0.348	0.370
0.740	0.746
6.263	6.104
0.500	0.500
29.886	-10
	1.522 0.624 0.348 0.740 6.263

Table 1: Model main dimensions

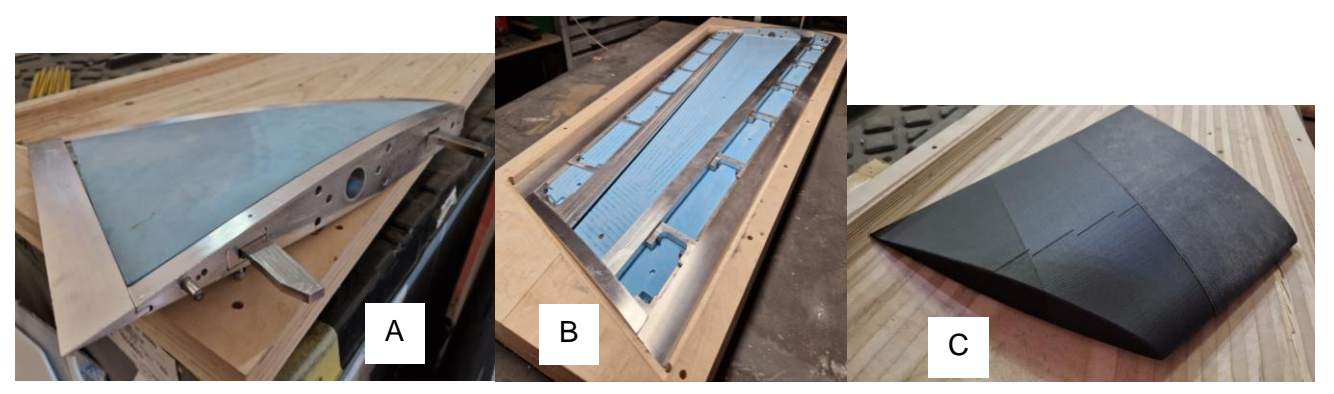


Figure 6: Three parts of the tailplane model.





Figure 7: Different tested LEX geometries.

2.3 Wind tunnel balance and instrumentation

While the "dummy" fuselage is attached to the test-section wall through several screws (so no force are measured on the fuselage), the tailplane model is mounted on an external balance which will measure lift, drag, pitching moment and bending moment (which can be used to highlight the spanwise position of the resultant of lift forces, also linked to the stall path at high angles of attack). The balance is composed of several load cells connected to a signal amplifier. The signals are acquired through a NI acquisition and analog to digital converter unit connected to a PC. The NI acquire signals from load cells, from a X-BOW tilt sensor which will measure angle of attack, from an high-accuracy pressure transducer which will measure dynamic pressure. The model is connected to an electric motor (mounted on the balance) that can change the angle of attack of the model though a very accurate rotation. Figure 8 shows the balance sketch, the and the rigid link between the model and the external balance.

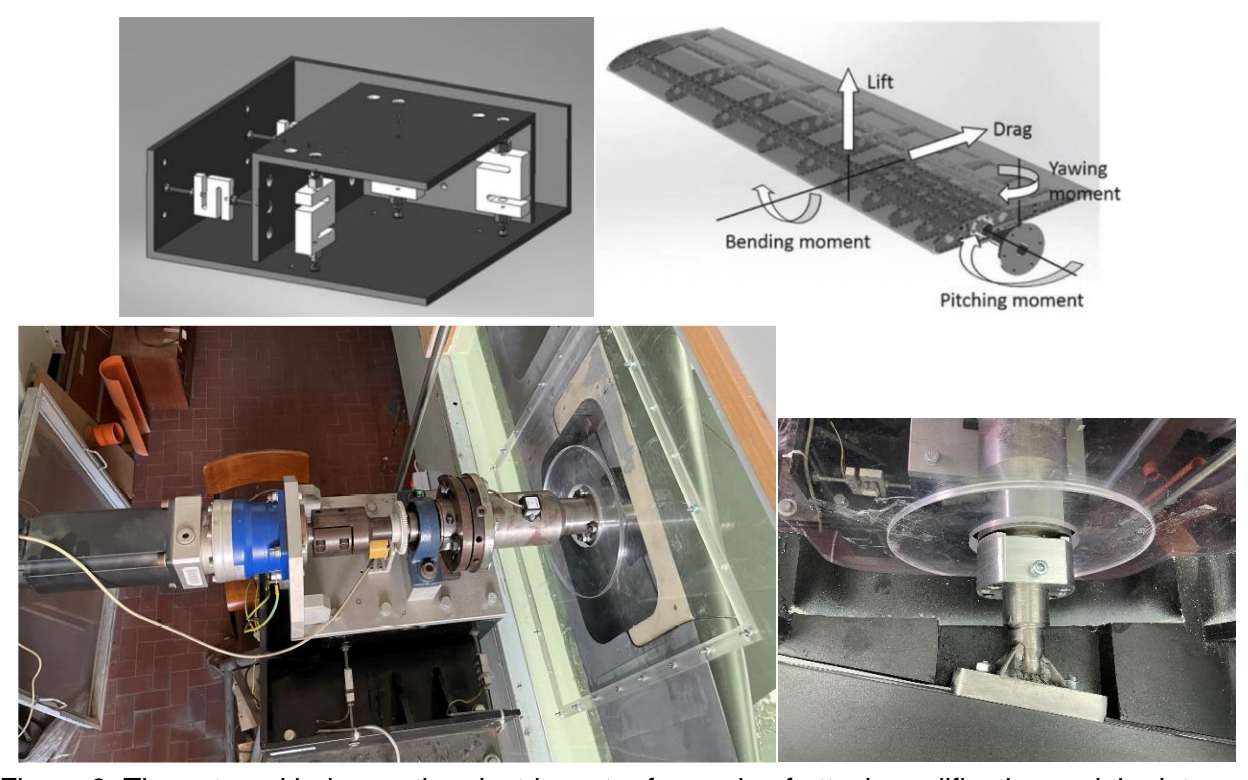


Figure 8: The external balance, the electric motor for angle of attack modification and the internal link to the tailplane model.

Table 2. External force balance characteristics and accuracy

Component	Range		Accuracy
	Min	Max	
Normal force (lift) L (Kgf)	-80	100	±0.030
Horizontal force (drag) D (Kgf)	-12	12	±0.005
Pitching moment M (Kgf·m)	-15	15	±0.010
Bending moment M_b (Kgf·m)	-40	60	±0.030
Yawing moment M_y (Kgf·m)	-8	8	±0.006

The balance has been accurately calibrated and forces are obtained from 5 load cells signals through a complex 5×5 calibration Matrix. For each test the offset is measured before test, allowing to measure only aerodynamic forces not considering the model weight. The pitching moment is

corrected for the modification of the model centre of gravity (so the model weight effect on pitching moment) while changing the angle of attack.

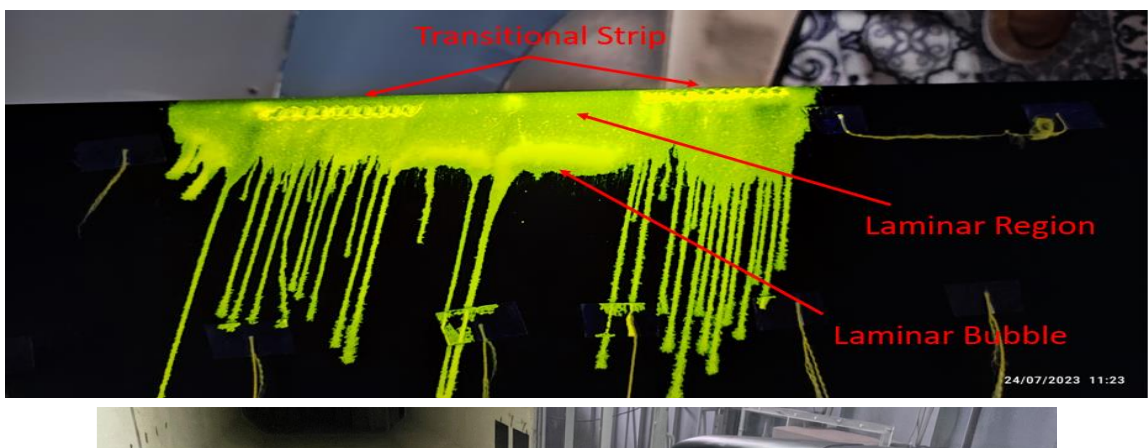
The dynamic pressure in the test section (to obtain aerodynamic coefficients from measured forces) is measured through a Venturi system and obtained through a calibration made with empty test section. The dynamic pressure has been measured with an accuracy of about 0.5 Pa (the tests have been performed at a speed of about 35 m/s with a dynamic pressure around 700 Pa. The X-BOW tilt sensor allows the measurement of the angle of attack with an accuracy of 0.02 deg.

To obtain the corrected aerodynamic coefficients, the dynamic pressure has been corrected for solid and wake blockage and the angle of attack, lift pitching moment and drag have been corrected for classical corrections (streamline curvature and upwash correction due to the wall effects).

3. Wind tunnel test results

3.1 Tests preparation

In order to test the model in fully turbulent conditions (also for appropriate possible scaling with Reynolds number) avoiding the laminar separation bubble (test Reynolds number referred to the mean chord is about 1 million) the tailplane has been equipped with a very thin aluminum zig-zag tape placed at the leading edge as transition promotion device. Several flow visualizations with fluorescent oil have been made to check the efficiency of the transition strip (see Figure 9).



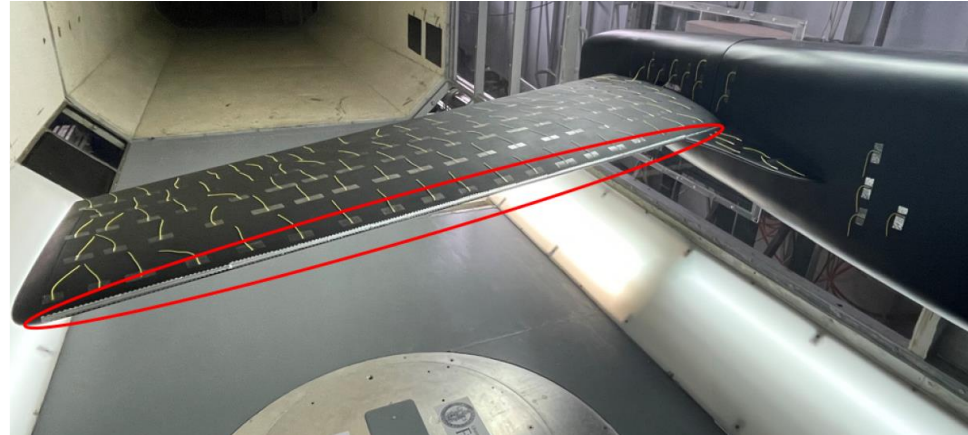


Figure 9: Flow visualization and transition strip effect. Alpha 5 deg.

Transition strip applied at the model leading edge.

3.2 Wind tunnel test results – positive backward sweep angle

The first tests have been performed on the model with classical configuration with positive sweep angle (see Figure 10). As it is well known, the positive swept tailplane at high angle of attack is characterized by a stall in the tip region. In order to check the effects of some possible stall control device, the model has been tested also with several boundary layer fences which should reduce the flow separation and affect the stall at the tip region. Figure 10 shows several fences that have been place along the tailplane span.









Figure 10: Positive sweep model and several boundary layer fences tested.

Tests results are shown in Figure 11. The boundary layer fences can lead to a light improvement of the maximum lift coefficient of the tailplane (10% improvement, from 0.70 to about 0.78) and a light delay in the stall angle (from 15 deg to 17 deg). The fence configuration with more efficiency is the configuration with 2 fences mounted on the model. The drag polar is not shown because it is not relevant for the results.

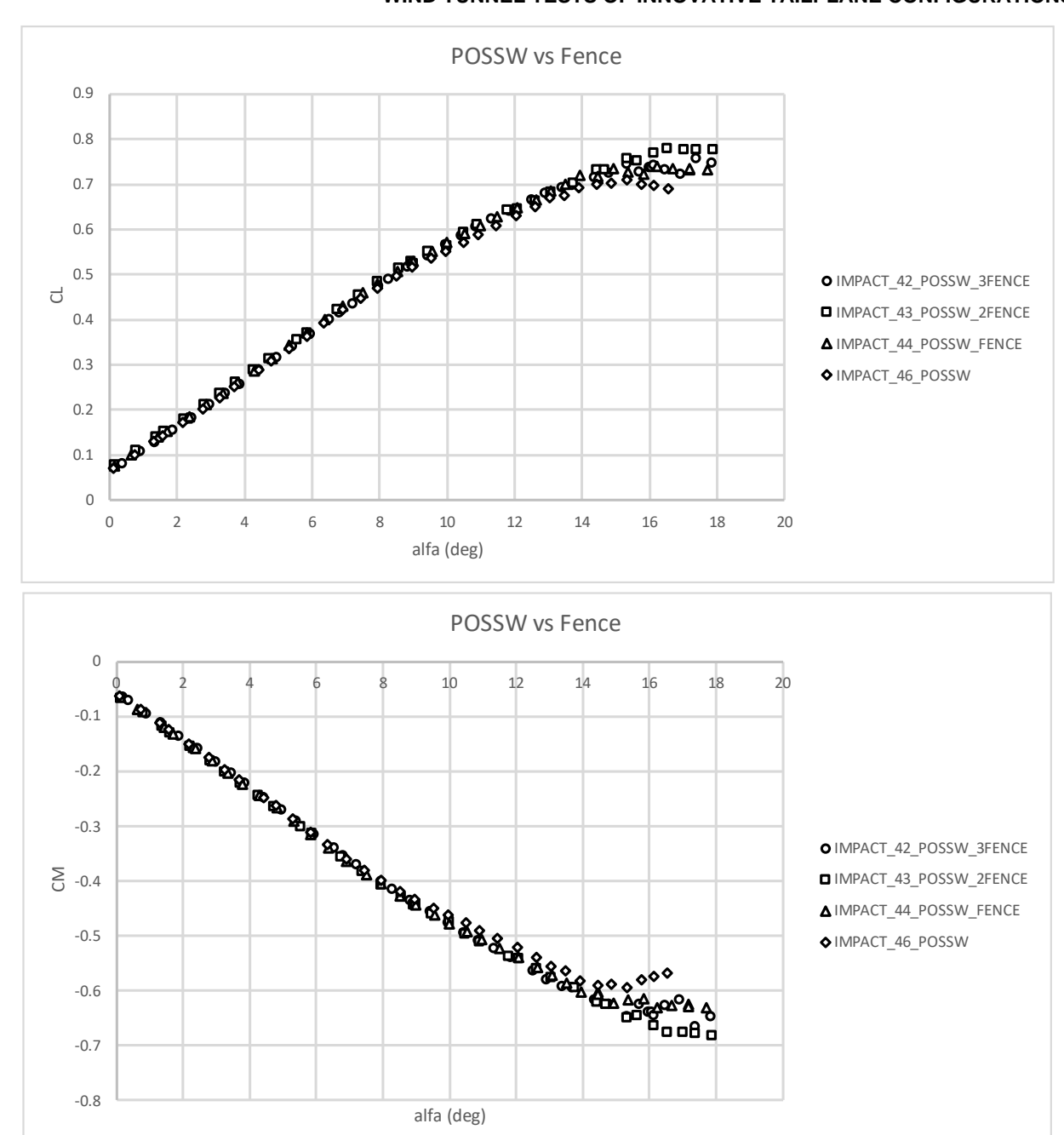
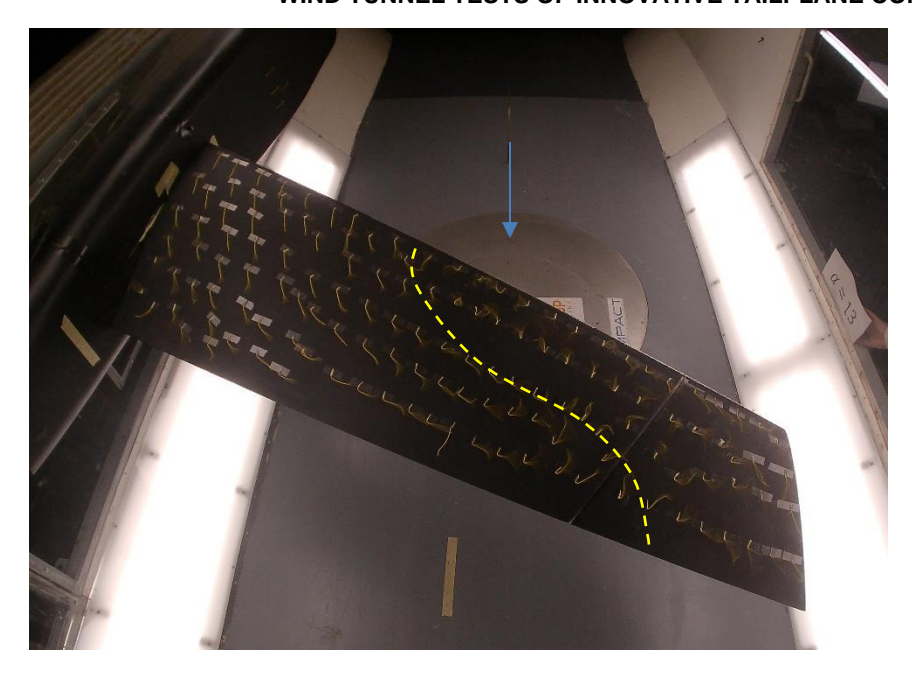


Figure 11: Positive sweep tailplane model wind tunnel test results. Lift coefficient and pitching moment coefficient. Wind speed V=35 m/s, Reynold =1 million, corrected angle of attack and coefficients.

Figure 12 shows some flow visualization through tufts at an angle of attack (corrected angle, as shown in Figure 11) of 14.3 deg. At that angle (stall condition for the tailplane), the tailplane model without fences shows a massive flow separation not only in the tip region, but also for more than 50% of the chord at 40-60% of the span. The two fences improve a little bit the flow separation in the tip region and on all the model, leading to a light increase of the lift coefficient (even more evident in the moment coefficient curve, see Figure 11).



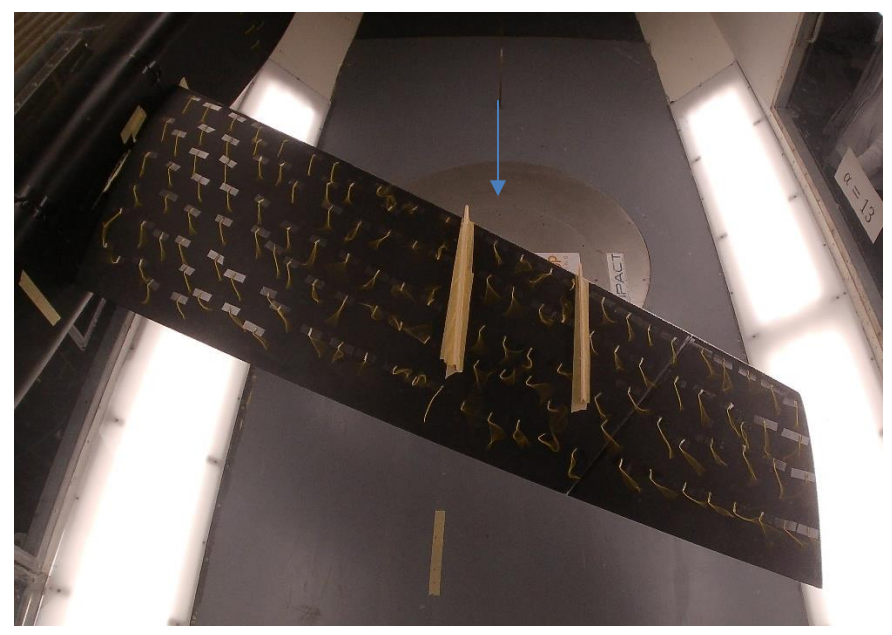


Figure 12: Flow visualization through tufts showing flow separation in the tip region at an angle of attack of 13 deg, corresponding to a corrected alpha of 14.3 deg.

3.3 Wind tunnel test results – forward swept tailplane model

The tailplane model with negative sweep angle (forward swept tailplane) also shown in Figure 9 has been tested at the same Reynolds number, without LEX device and with the previous 5 different LEX mounted on the model. The following figures shows the aerodynamic results. In Figure 13 a comparison between the configuration with forward sweep and that one with conventional backward sweep is shown. The different sweep angles (-10° for the forward swept case and +30° for the positive swept case) lead to a slightly different lift curve slope. The lift curve slope is 0.0517 1/deg for the positive sweep case and 0.0577 1/deg for the forward sweep case. Also the maximum lift coefficient is slightly higher for the forward swept case (0.75 for the forward swept case and 0.71 for the backward swept case).

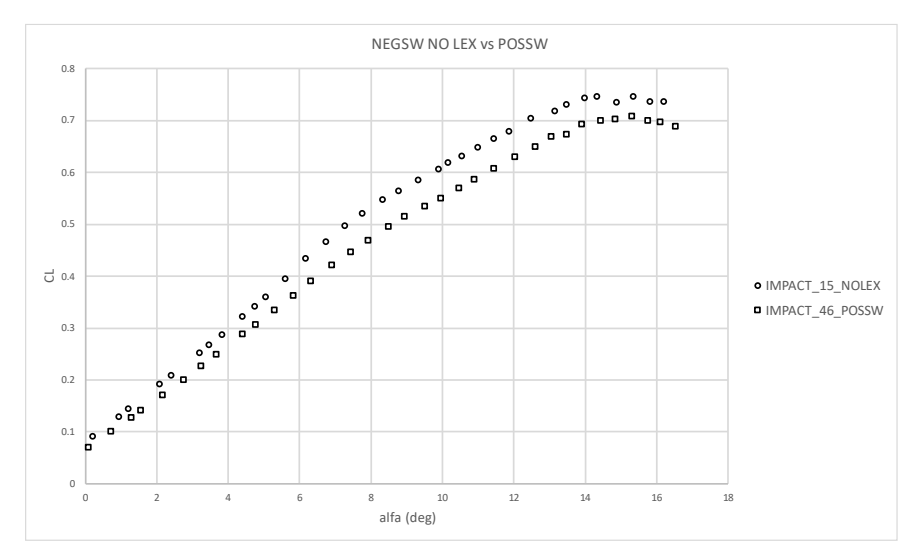


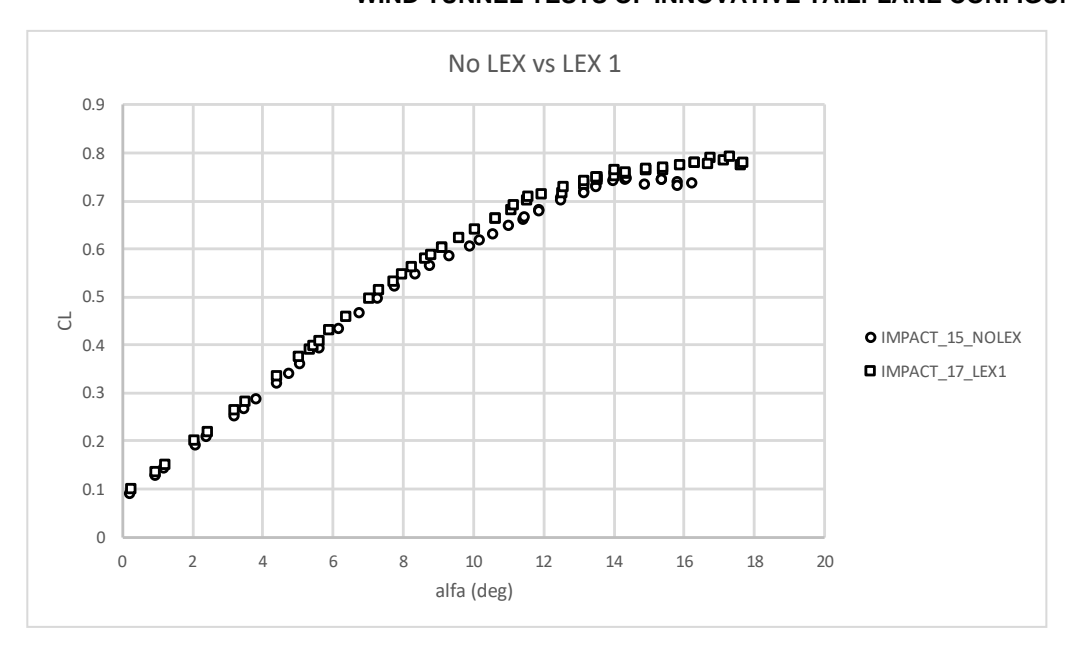
Figure 13: Forward swept case vs positive backward swept case.

Tests at V=35 m/s and Reynolds =1 million.

The forward swept case at stall conditions shows flow separation at the root, as it is expected. Several tests have been made with the forward swept tailplane with the application of the LEX devices shown in previous part (see Figure 7) with the intent of controlling the flow separation in the root region (close to the fuselage) increasing the maximum lift coefficient. Figure 14 shows the results in terms of lift coefficient curve and moment coefficient curve with and without the first LEX device (LEX n. 1, see Figure 7) installed on the model.

It is fully evident from the lift coefficient curve and even more from the moment coefficient curve that the LEX leads to an improved flow separation and an higher maximum lift coefficient. The effects are quite evident only at angles of attack higher than 5-6 deg. The lift slope in the linear range is almost unchanged w.r.t. the case without LEX. The coefficients are referred to the original tailplane area shown in Table 1, so a small increment it is also due to the vortex lift produced by the LEX itself.

However, being the LEX area very small (only 3% in average) compared to the tailplane model area and being the aerodynamic effects (increment in maximum lift coefficient) almost 10%, it is evident that the main effects of the LEX is due to the positive interference on the tailplane. In particular the LEX at high angles of attack (higher than 4-5 deg) produces a vortex which contributes to control flow separation in the tailplane root region. The vortex produced leads basically also to an induced angle of attack which is negative inboard (reducing flow separation in the root region close to the fuselage) and higher immediately outboard. This leads to a shift of the separated region outboard in spanwise direction, improving the maximum lift coefficient of the tailplane.



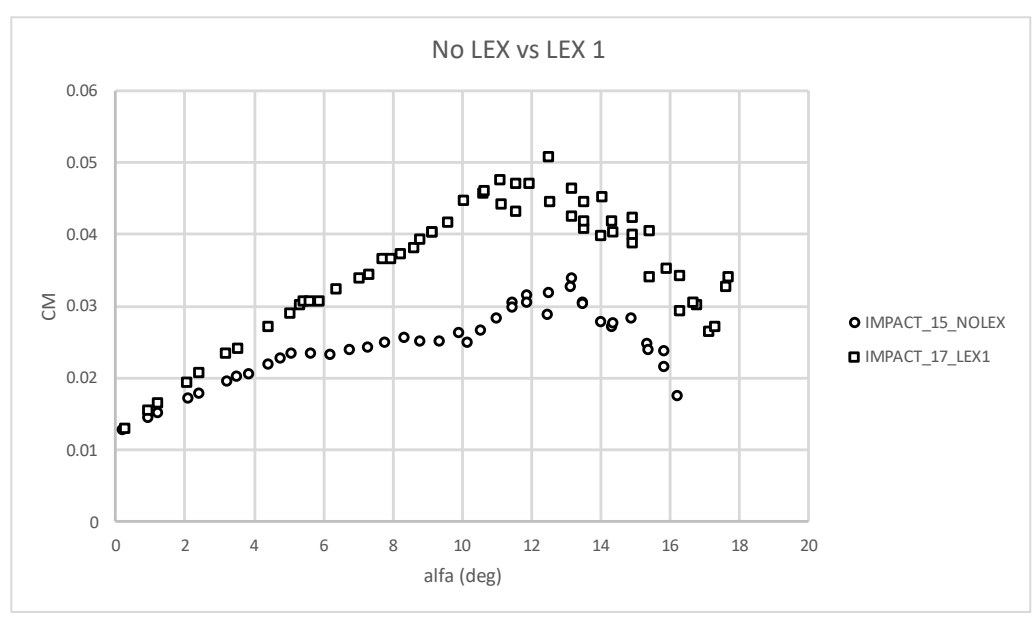


Figure 14: Forward swept tailplane wind tunnel test results without Lex and with LEX n. 1 (see Figure 7). V=35 m/s, Reynolds = 1 million.

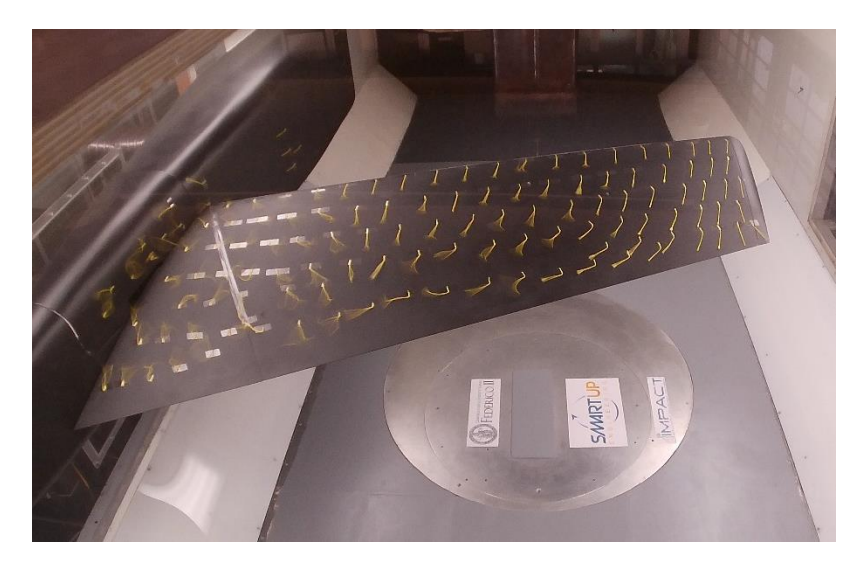
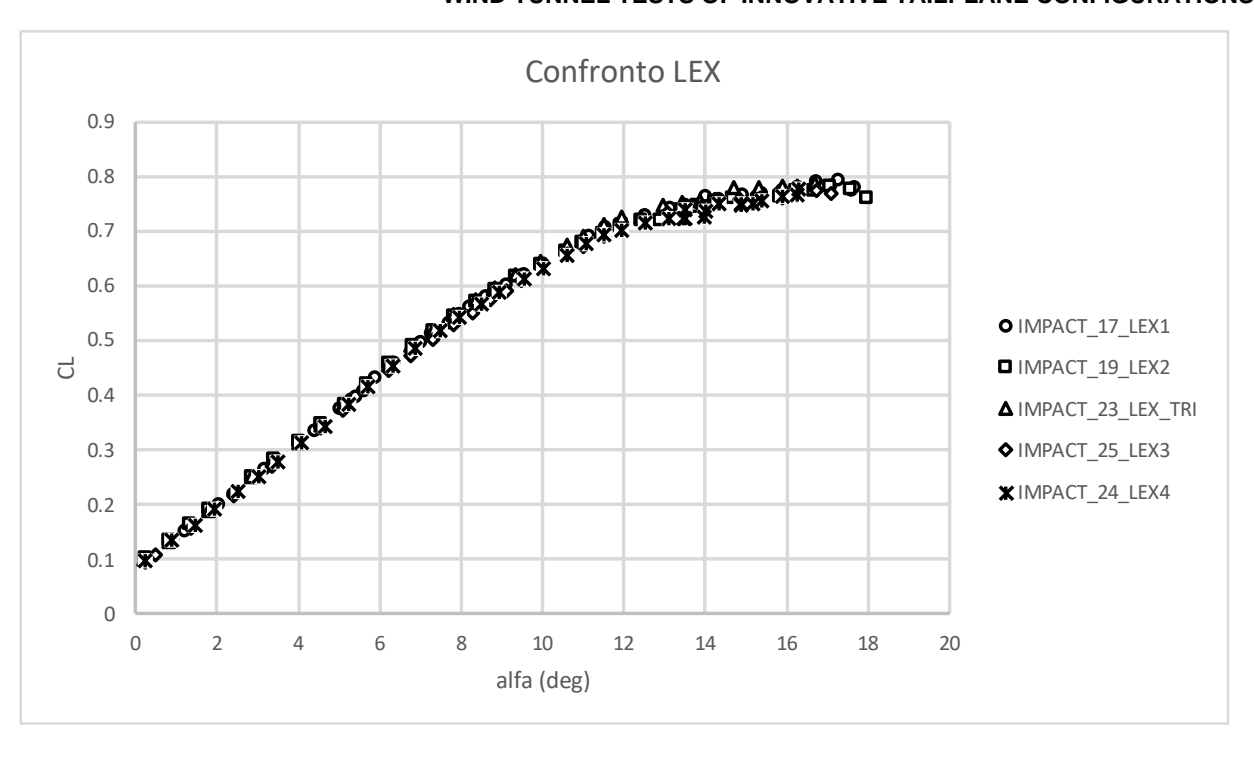




Figure 15: Forward swept tailplane. Flow visualization through tufts. Tailplane without LEX (upper image) vs Tailplane with LEX n. 1 installed. Angle of attack of about 13 deg.

3.4 Effect of different LEX devices – forward swept tailplane model

Wind tunnel tests have been made with different LEX installed (LEX geometries shown in Figure 7). Figure 16 shows the results obtained. All the LEX geometries lead to an improvement of the flow separation and an increment of the maximum lift coefficient.



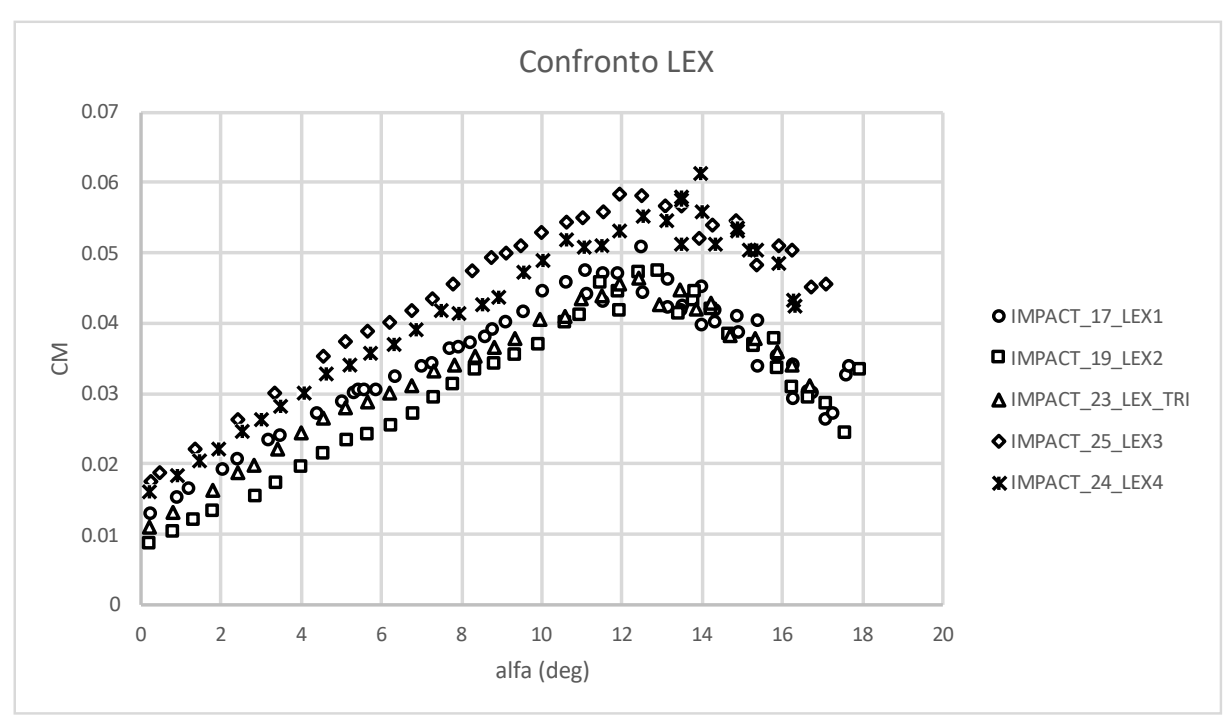


Figure 16: Lift coefficient curve and moment coefficient curve of the forward swept tailplane with all different LEX devices installed. V=35 m/s.

4. Conclusions

The conducted wind tunnel tests on innovative tailplane configurations with forward sweep and Leading Edge Extension (LEX) devices have yielded significant insights. The results demonstrate that the forward swept tailplane with LEX devices effectively controls flow separation at the root region, enhancing the maximum lift coefficient. The LEX devices produce a vortex at high angles of attack, which mitigates flow separation and shifts the separated region outboard, thereby improving overall aerodynamic performance. These findings underscore the potential of unconventional tailplane geometries to meet the dual objectives of reducing emissions and enhancing fuel efficiency, aligning with the broader goals of sustainability in the aerospace sector.

5. Archiving

The ICAS 2024 proceedings will receive an ISBN number and will be cataloged and archived by the German National Library.

6. Contact Author Email Address

mailto: fabrnico@unina.it

7. Copyright Statement

The authors confirm that they, and/or their company or organization, hold copyright on all of the original material included in this paper. The authors also confirm that they have obtained permission, from the copyright holder of any third party material included in this paper, to publish it as part of their paper. The authors confirm that they give permission, or have obtained permission from the copyright holder of this paper, for the publication and distribution of this paper as part of the ICAS proceedings or as individual off-prints from the proceedings.

References

- [1] R.M. Arnaldo Valdes RM, S. Burmaoglu S, Tucci V, Braga da Costa Campos LM, Mattera L, Gomez Comendador VF. Flight path 2050 and ACARE goals for maintaining and extending industrial leadership in aviation: a map of the aviation technology space. *Sustainability* Vol. 11 (7) (2019) 2065, https://doi.org/10.3390/su11072065.
- [2] Cusati V, Corcione S, Memmolo V. Potential Benefit of Structural Health Monitoring System on Civil Jet Aircraft. *Sensors* 2022; Vol. 22(19):7316 https://doi.org/10.3390/s22197316
- [3] Cusati V, Corcione S, Memmolo V. Impact of Structural Health Monitoring on Aircraft Operating Costs by Multidisciplinary Analysis. *Sensors* 2021; 21(20):6938 https://doi.org/10.3390/s21206938
- [4] Krone N Jr. Forward swept wing flight demonstrator. Aircraft Systems Meeting, 1980, p. 1882.
- [5] Weisshaar TA. Aeroelastic stability and performance characteristics of aircraft with advanced composite swept forward wing structures. *Tech. Rep.*, *Virginia Polytechnic Inst and State Univ Blacksburg Dept of Aerospace and Ocean Engineering*, 1978.
- [6] Weisshaar TA. Aeroelastic tailoring of forward swept composite wings. *Journal of Aircraft*. Vol. 18 (8) (1981) 669–676, https://doi.org/10.2514/3.57542.
- [7] Hertz T, Shirk M, Ricketts R, Weisshaar T, Aeroelastic tailoring with composites applied to forward swept wings. Technical Report, *Air Force Wright Aeronautical Labs Wright-Patterson* AFB OH, 1981.
- [8] Krone N Jr. Divergence elimination with advanced composites. *Aircraft System and Technology Meeting*, 1975, p. 1009.
- [9] Weisshaar TA. Divergence of forward swept composite wings. 20th Structures, Structural Dynamics, and Materials Conference, 1979, p. 722.
- [10] Shirk MH, Hertz TJ, Weisshaar TA. Aeroelastic tailoring-theory, practice, and promise. *Journal of Aircraft*. Vol. 23 (1) (1986) 6–18, https://doi.org/10.2514/3.45260.
- [11] Wunderlich T, Reimer L. Integrated process chain for aerostructural wing optimization and application to an NLF forward swept composite wing. *AeroStruct: Enable and Learn How to Integrate Flexibility in Design*, Springer, 2018, pp. 3–33.
- [12] IMPACT Clean Sky Project, https://www.impact-cleansky-project.eu
- [13] Corcione S, Mandorino M, Cusati V. An integrated aerostructural optimization approach for innovative tailplane configurations. *Aerospace Science and Technology* (2024), Volume 150, 2024, 109242, ISSN 1270-9638, doi.org/10.1016/j.ast.2024.109242
- [14] Llamas Sandín RC, Luque Buzo, M, (2013). Aircraft Horizontal Stabilizer Surface (Patent US 8,360,359 B2). AIRBUS
- [15] M. K. T. W. J. B. L. H. Seitz, The dlr project lamair: Design of a nlf forward swept wing for short and medium range transport application, in 29th AIAA Applied Aerodynamics Conference, Honolulu, Hawaii, 2012.
- [16] A. H. A. & R. K. Seitz, "The DLR TuLam project: design of a short and medium range transport aircraft with forward swept NLF wing.," CEAS Aeronautical Journal, p. 449–459, 2020.
- [17] Roskam J. Airplane Aerodynamics and Performance. Lawrence, Kansas: DAR corporation, 1997.